Available online at www.sciencedirect.com
SCIENCE DIRECT
Journal of the European Ceramic Society 26 (2006) 2743–2751
www.elsevier.com/locate/jeurceramsoc

Cellulose acetate based gelcasting process for Gd-containing ceramic bodies

Achim Müller*, Fayou Yu, Monika Willert-Porada

Chair of Materials Processing, University of Bayreuth, Universitätsstr. 30, FAN-C, D-95440 Bayreuth, Germany

Received 11 February 2005; received in revised form 20 July 2005; accepted 31 July 2005
Available online 4 October 2005

Abstract

A new route of gelcasting is applied to prepare Gd_2O_3 and Gd_2O_2S as well as Al_2O_3 ceramic parts, i.e. thin plates and fibres. Cellulose acetate is used as monomer. Instead of a water-based solvent system, ethylenediamine as solvent is employed; therefore, moisture- and air-sensitive ceramic powders can be processed, such as Gd_2O_2S. The presented work focuses on the characterisation of the slurry by rheological and chemical measurements, the polymerisation process and the first results of the fabrication of ceramic bodies. Both green and sintered parts were investigated using electron microscopy, X-ray diffractometry and physisorption.

Keywords: Fibres; Gd_2O_3; Al_2O_3; Shaping

1. Introduction

Gelcasting is an innovative forming method for fabricating ceramic bodies by means of an in situ polymerisation, through which a macromolecular 3D-network is created to hold the ceramic particles together. This polymer based fabrication method offers great advantages to form various body shapes in comparison to dry processing. Numerous articles were already published about gelcasting methods (e.g.[1–8]). However, the majority of known gelcasting routes use water-based systems, i.e. the solvent for the monomer is water. Non-aqueous systems are not often reported in detail in the literature.[9,10] Particularly for moisture sensitive green-bodies, such methods are therefore not applicable. There are two reasons for developing the new system: (1) water free for non-oxide ceramics and (2) Polymerisation with a "low carbon" content polymer and an initiator system, which does not introduce other metal ions than the ceramic ones. Furthermore, not much is known about the possibility to prepare ceramic fibres via a gelcasting route. This article discusses both the results for the preparation of ceramic bodies using a non-aqueous gelcasting method and the possibility of making fibres. The method is based on ethylenediamine (EDA) as solvent, in which cellulose acetate (CA) as the monomer is dissolved. Due to the strong base (EDA)[11] a partial deacetylation occurs and CA becomes soluble. The ceramic powder is dispersed into the solution. Controlled gelation and polymerisation is achieved by adding metal cations as initiator to the slurry, via a solution of appropriate salts in EDA or acetone. The latter solvent is furthermore used to control the polymerisation process and the viscosity of the slurry. Since the gelcasting method is suitable for all kinds of shaped bodies, it is a challenge to extrude slurries through a filament and draw ceramic fibres. We present different examples for the non-aqueous gelcasting route, the processing into special thin plate shape for a specific application and show an outline how to prepare ceramic fibres by this route.

2. Experimental

The experiments were done with Gd_2O_3 (ChemPur, 99.9%), Gd_2O_2S (Med CTD Siemens) and Al_2O_3 (A16 SG, Alcoa) ceramic powders. Gd_2O_2S is a widely used ceramic for scintillator detectors (e.g.[12–14]). Especially for metal oxysulfides it is essential to work in a moisture-

* Corresponding author. Tel.: +49 921 557207; fax: +49 921 557205.
E-mail address: Achim.Mueller@uni-bayreuth.de (A. Müller).

0955-2219/$ – see front matter © 2005 Elsevier Ltd. All rights reserved.
doi:10.1016/j.jeurceramsoc.2005.07.057

Table 1
Composition of different slurries for the gelcasting process

	wt.% CA in EDA	vol.% Ceramic	wt.% Initiator
GOS	5.3	25.4	1
Gd_2O_3	5.3	25.0	1
Al_2O_3	5.3	25.0	1

and air-free environment, because the oxysulfide can easily transform to a metal sulphate.[15] About 5 wt.% of cellulose acetate (CA, Sigma–Aldrich) is dissolved under continuous stirring (torsional stirrer at 500 min^{-1}) in 5 ml ethylenediamine (EDA, Merck, >99%). After completion ca. 25 vol.% of the dried ceramic powder is added (Table 1). When it is completely dispersed 1 wt.% of Gd-acetate ($Gd(O_2CCH_3)_3{\cdot}xH_2O$, ChemPur, 99.9%) or 1 wt.% basic aluminium acetate ($Al(CH_3CO_2)OH$, Sigma–Aldrich) in EDA, respectively, is added to the slurry to activate the gelation and polymerisation step. By adding a small volume (between 0.02 and 0.14 vol.%) of acetone (Merck, maximum amount of H_2O: 0.01%), one can control both the onset of the gelation and the viscosity of the slurry. Immediately after mixing the slurry, the complete volume (about 5 ml) is casted into a mould or extruded through a filament to draw fibres. The results presented in the following are from preliminary experiments using a 5 ml syringe as "extruder tool".

The Gd_2O_3 and Al_2O_3 ceramic bodies are debindered at 700 °C in air with a heating rate of 30 K/h and sintered at a temperature of 1700 °C for 2 h (to form quite dense bodies) in air with a heating rate of 200 K/h in one cycle. The Gd_2O_2S plates are debindered first in a tube furnace at 320 °C for 20 min in air with a heating rate of 60 K/h and then heated up to 700 °C in an argon atmosphere for 1 h, with the same heating rate of 60 K/h. The debindered Gd_2O_2S is sintered at 1400 °C for 2 h in a nitrogen gas atmosphere.

The gelcasting process was designed according to viscosity measurements (Physica MCR500 rotational rheometer) and NMR investigation (Bruker AC, 250 MHz). Physisorption measurements on green, debindered and sintered parts were done using Hg-intrusion (Micromeritics AutoPore III) and pore size distribution calculations using the method of Brunauer–Emmet–Teller, BET (Micromeritics ASAP 2010). Hardness determination was done with a Buehler macro-Vickers tester, type 2104.

For further characterisation X-ray diffractometry (Philips X'Pert PW3040), optical light microscopy (Olympus SZ X12) as well as scanning electron microscopy (Jeol 840 A) was used. X-ray measurements were taken with Cu Kα ($\lambda_{\alpha1} = 0.154056$ nm; $\lambda_{\alpha2} = 0{\cdot}154439$ nm) radiation subtracting the α2 parts with the analysis software. The used average accelerating voltage for the SEM pictures was 20 kV. In some cases it was necessary to reduce the voltage due to local charging. The samples were sputtered with gold to make them conductive.

3. Results

The volumetric ratio of the ceramic powder has an influence on the gelation behaviour. Rheologic measurements were undertaken to investigate the behaviour of ceramic powder load on the viscosity of the slurry.[16] Fig. 1a and b show the data for the viscosity of Gd_2O_2S and Al_2O_3 slurries as function of ceramic powder content. These slurries for the viscosity measurements contain ceramic powder suspended in *N*,*N*-dimethylacetamide (DMA). EDA ($\rho = 1{,}457$ g/cm^3) is rather volatile and corrosive for the measurement, but the properties like the density of DMA ($\rho = 1{,}437$ g/cm^3) are nearly the same.

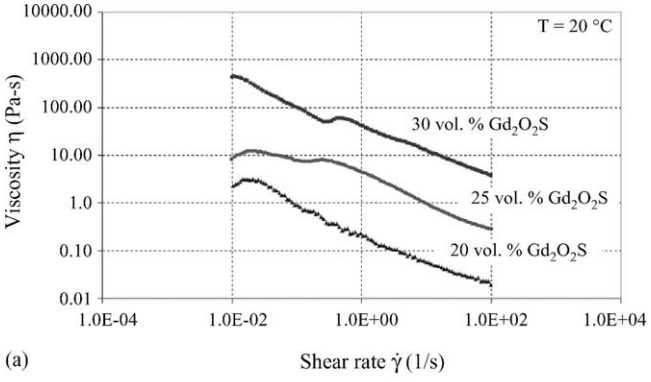

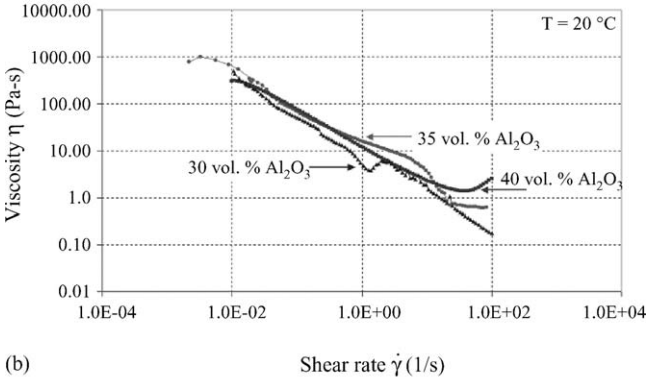

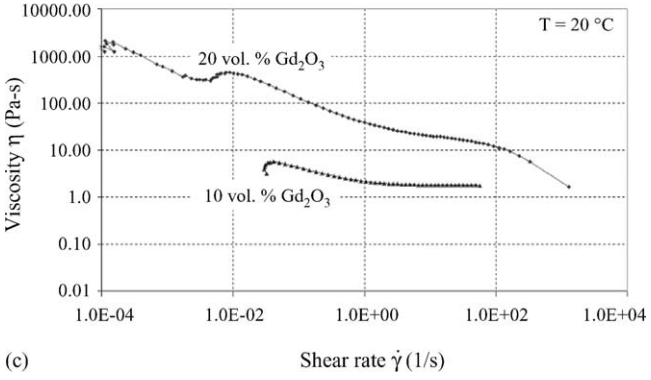

Fig. 1. (a and b) Viscosity of Gd_2O_2S and Al_2O_3 slurries in DMA as function of ceramic powder content, measured with a rotational rheometer. (c) Viscosity of Gd_2O_3 slurries in DMA as function of ceramic powder content, measured with a rotational rheometer.

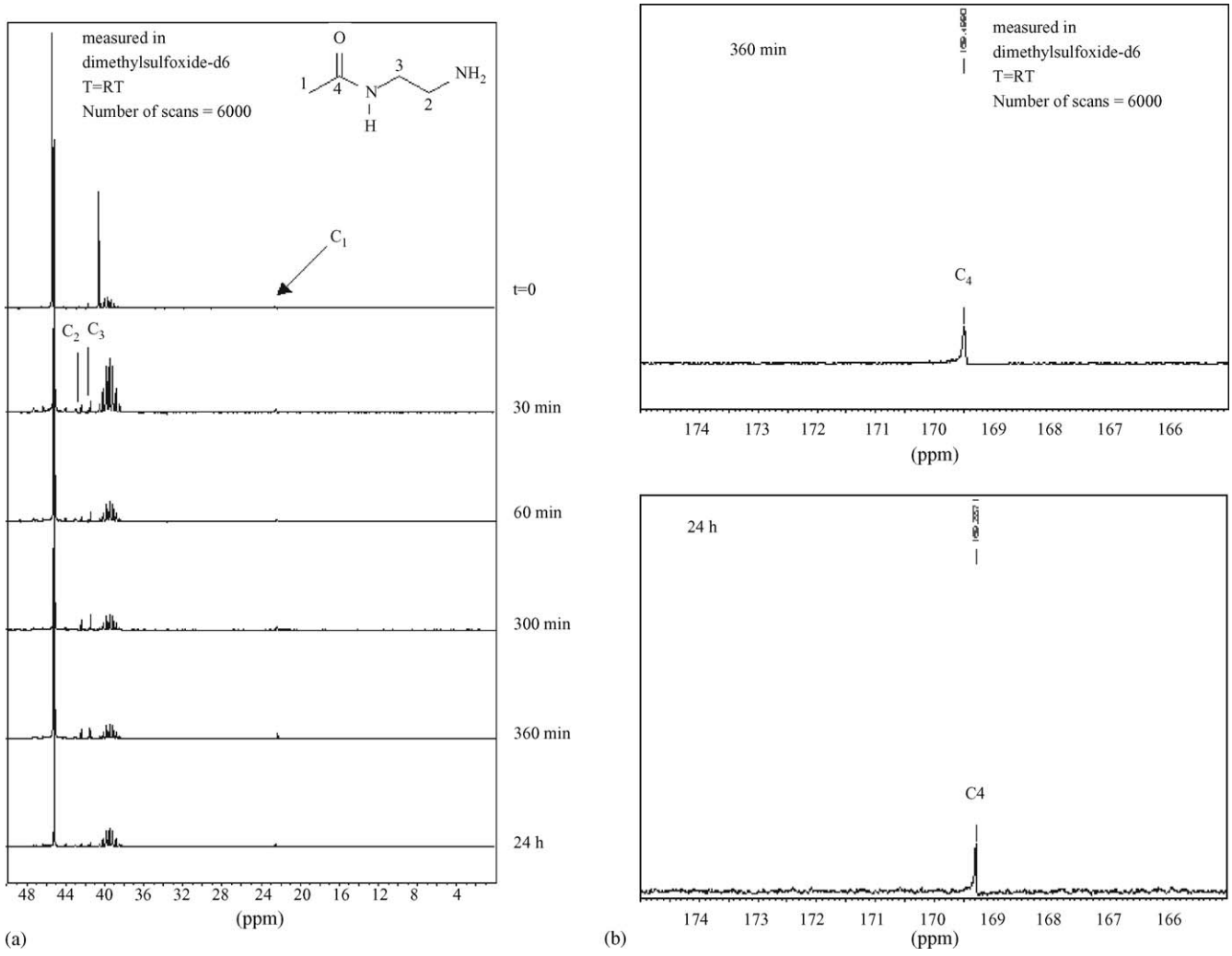

Fig. 2. (a) ^{13}C NMR of the liquid released from the CA/EDA gel as function of time, chemical shift 4–48 ppm. (b) ^{13}C NMR of the liquid released from the CA/EDA gel as function of time, chemical shift 166–174 ppm.

The increase of viscosity with increasing powder load is rather steep especially for a Gd_2O_2S slurry, whereas the viscosity of an Al_2O_3 mixture does not change much with increasing powder volume fraction. The viscosity of Gd_2O_3 ceramic slurry including the initiator is shown in Fig. 1c. All gelcast slurries show similar effects, where the increase of η is rather steep with higher powder load.

By ^{13}C NMR measurements the mechanism of CA swelled and dissolved in EDA as function of time was monitored. The concentration of CA is lower than for the slurry preparation due to measurement requirements. The spectra are taken from the liquid released (supernatant) from the CA gel. The data are shown in Fig. 2a for the chemical shift region between 4 and 48 ppm, and in Fig. 2b for the region from 166 to 174 ppm. The C(4) atom from the acetyl-group can be observed the first time in a sample measured after 270 min of agitation. This is the time, where the gelation starts, and therefore, the C(4)-signal is an indicator for the deacetylation. For clarity only the NMR data for the 300 min and 24 h scaling time are shown in Fig. 2b.

The characteristics of different concentrations of cellulose acetate dissolved in EDA are shown in Fig. 3. The stability time is defined by the visual observation when the mixture turns from a transparent into either a turbid suspensions or

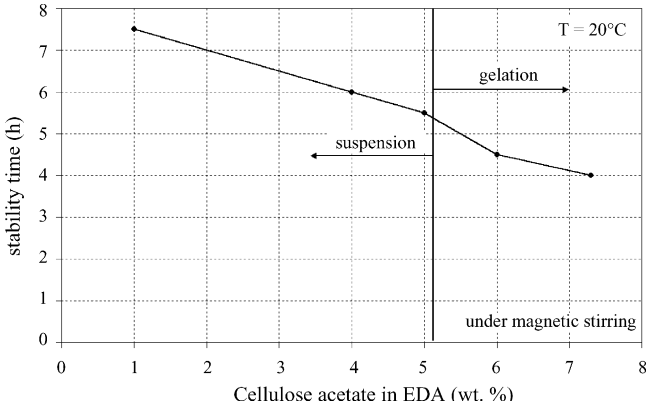

Fig. 3. Gelation behaviour of CA in EDA as function of concentration.

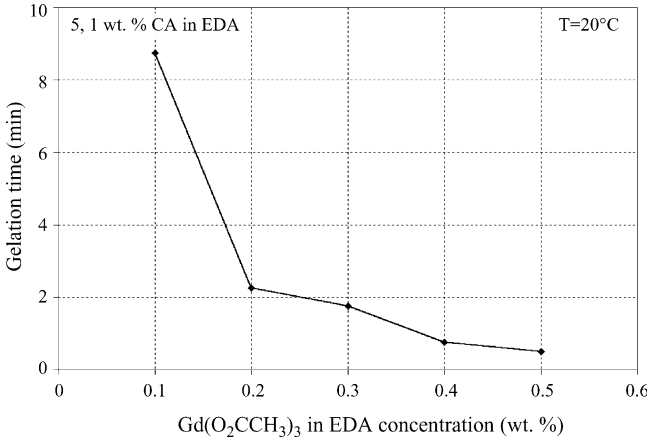

Fig. 4. Gelation time of CA solution in EDA as function of $Gd(O_2CCH3)_3$ in EDA concentration.

an opaque polymer. The higher the concentration of CA the shorter the time needed for polymerisation occurs. However, a defined amount of CA is necessary for a gelation to take place. The diagram shows clearly that for around 5.1 wt.% CA in EDA, a reasonable time to concentration ratio is given.

Investigations were done both with Gd_2O_3 and Gd_2O_2S in terms of the polymerisation with Gd^{3+}-ions ($Gd(O_2CCH_3)_3$) as initiator. Fig. 4 shows[16] that above a defined concentration of initiator the gelation time remains nearly constant. Further experiments prove that even with very high concentrations of gadolinium acetate, e.g. 30 wt.% $Gd(O_2CCH_3)_3$ in EDA, the polymerisation begins within less than 1 min, but not faster than for 0.5 wt.%.

The higher the content of ceramic powder the faster the gelation takes place, as shown in Fig. 5, but the time reaches a constant level as well. The ceramic powder load was limited in the experiments to obtain an appropriate time window for processing. Therefore, the maximum powder load was 40 vol.% for Al_2O_3, 25 vol.% in the case of Gd_2O_3, and 30 vol.% for Gd_2O_2S, respectively. The maximum achievable powder weight fraction is different due to different ζ-potentials for such powders and/or different grain sizes and

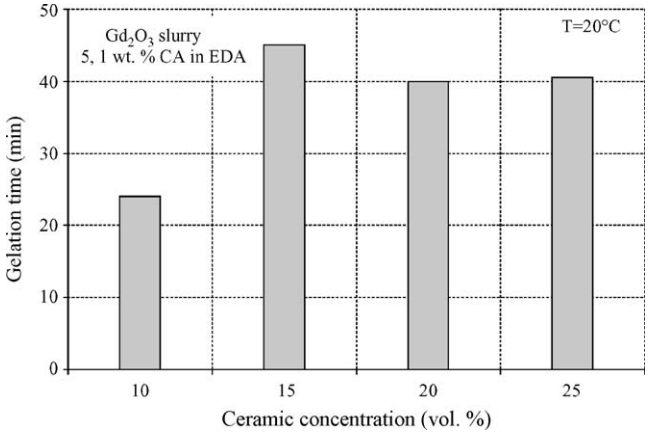

Fig. 5. Gelation time of Gd_2O_3 slurries as function of volume percentage.

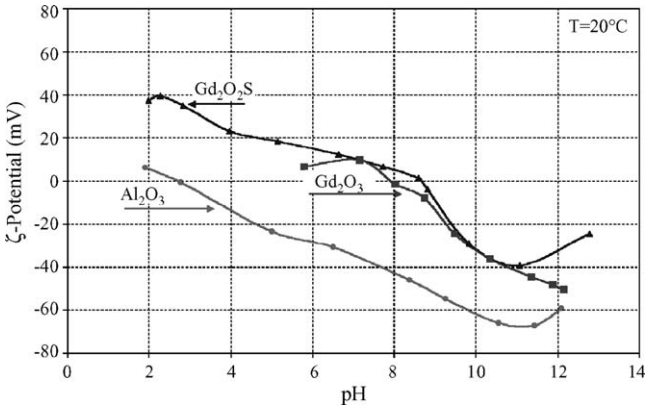

Fig. 6. ζ-Potentials for different ceramic powders as function of pH, measured in an electrolyte solution (0.001 M $NaNO_3$).[16]

their distribution. Measurements of the ζ-potential (Fig. 6) show lower values for Al_2O_3 than for Gd_2O_2S and Gd_2O_3, respectively.[16] The isoelectric point (IEP, at 0 mV) is located at pH 8.7 for Gd_2O_2S, 8.0 for Gd_2O_3 and 2.6 for Al_2O_3. The values of ζ-potential suggest that the surface of Gd_2O_2S is basic. Negative ions are adsorbed on the particle surface if pH >8.7. To obtain a stable suspension, the powder should be processed in basic conditions.

Concerning the control of the slurry viscosity, we investigated the behaviour in terms of adding acetone before the gelation starts. Fig. 7 shows the effect of adding different amounts of both technical pure and distilled acetone to slurries with different ceramic powders and concentrations. Above an acetone volume of 0.06 vol.% the increase in polymerisation time is rather steep for all ceramic powders. However, the time factor between Al_2O_3 and Gd_2O_3 slurries is approximately 3.5 with an alumina gel. With increasing acetone amount the polymerisation time for both Gd_2O_3 and Gd_2O_2S is further delayed, but the polymerisation time for Al_2O_3 is much more rapid compared to Gd_2O_3 slurry and reaches at 0.08 vol.% a constant level.

The casting process was performed with slurries of the composition shown in Table 1.

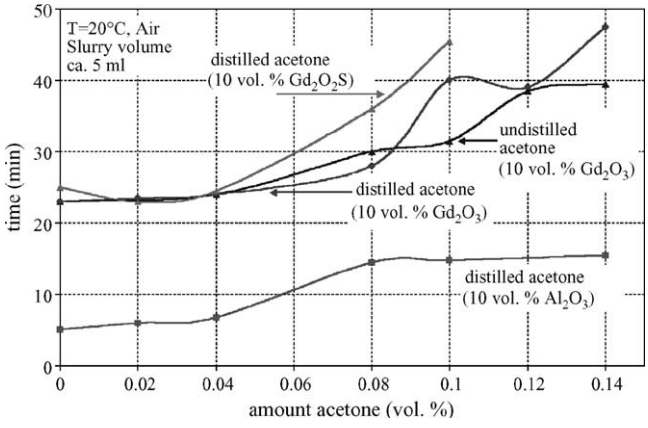

Fig. 7. Time effect of adding different volumes of acetone on the polymerisation of ceramic powder slurries.

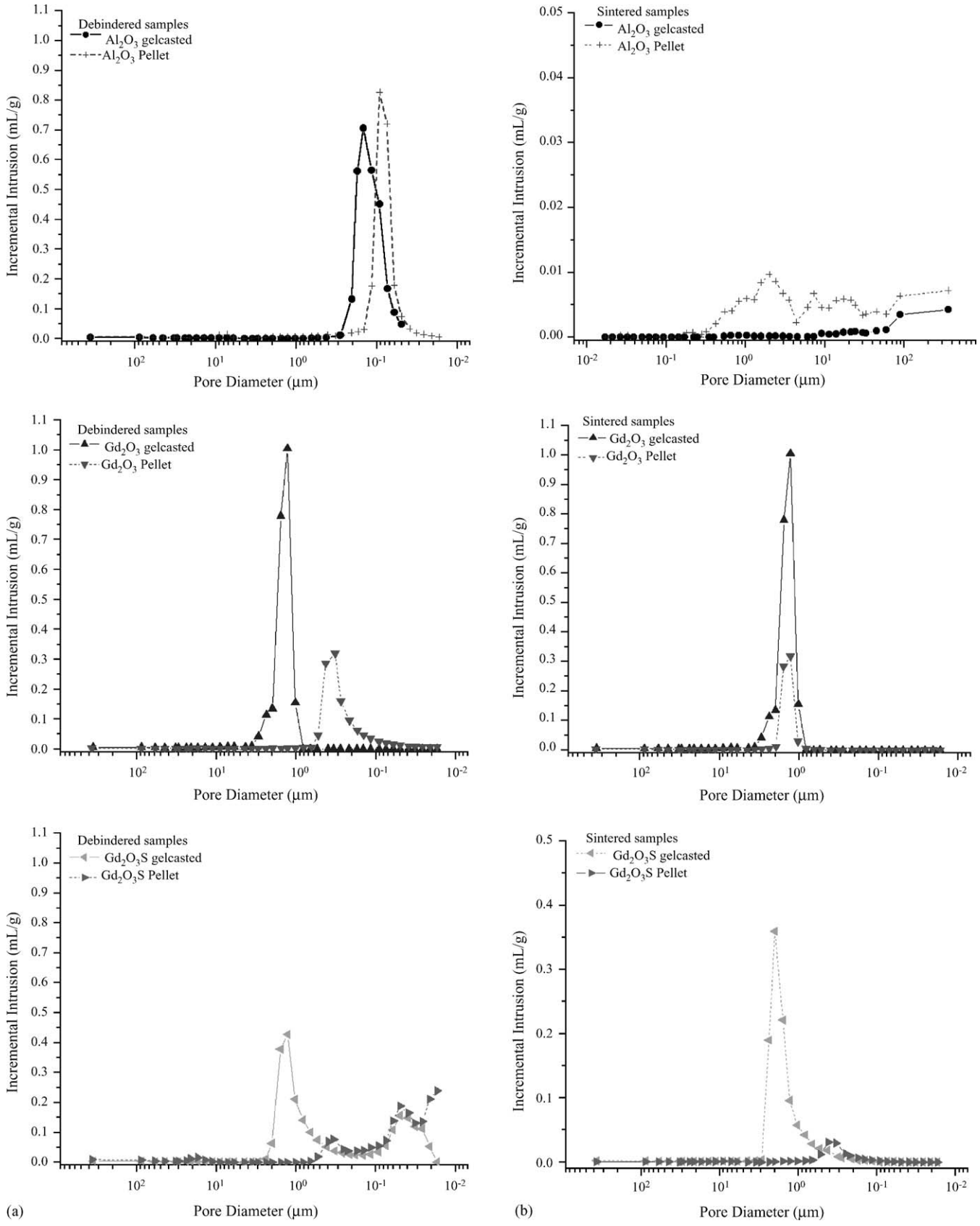

Fig. 8. (a) Data of the mercury intrusion showing the incremental intrusion vs. the pore diameter for different debindered samples. (b) Data of the mercury intrusion showing the incremental intrusion vs. the pore diameter for different sintered samples.

Table 2
Green density and pore size distribution of dried gelcast plates and uniaxially pressed pellets

	Green density (g/cm^3)	Average pore diameter by BET (nm)
GOS (gel)	6.49	21.6
Gd_2O_3 (gel)	4.07	9.6
Al_2O_3 (gel)	3.40	14.7
GOS (pellet)	6.43	18.1
Gd_2O_3 (pellet)	6.79	14.1
Al_2O_3 (pellet)	3.67	14.8

Experiments were done both by mixing the initiator with the slurry before filling the mould and by adding an initiator in EDA solution to the slurry already deposited in the mould. Table 2 shows the green densities and the average pore diameter of gelcast parts in comparison with uniaxially pressed pellets with a diameter of 13 mm. The results in terms of Vickers hardness of sintered samples are listed in Table 3. The difference is particularly significant for the Gd_2O_2S samples. The pellet shows a 10 times higher hardness than the gelcast sample. Table 4 lists the different densities of sintered samples. The differences in density and porosity of the gelcast and pellet samples are quite significant for Gd_2O_2S, but much smaller for Gd_2O_3 and especially Al_2O_3. To compare the debindered gelcast samples with uniaxially pressed ones as well as with sintered samples, in Fig. 8a and b the incremental intrusion (mercury) versus the pore diameter is plotted. The smaller the volume of intruded mercury is the less open pores exist in the sample. Differences can be seen for debindered samples. The pore diameter of Al_2O_3 pellets and the gelcast plate are rather similar. However, the Gd_2O_3 pellets show smaller pore diameters of one magnitude than the equivalent plates. A clearer difference can be observed for the Gd_2O_2S samples where the difference between pellets and plates is almost two magnitudes. The differences in mercury intrusion volume of sintered Al_2O_3 bodies are negligible. In the case of Gd_2O_3 the pore diameter is the same, but the Hg volume is higher for the gelcast sample. In the case of Gd_2O_2S, the gelcast sample shows larger pore diameters of one decade and a higher amount of intruded mercury.

Table 3
Hardness of sintered samples

Hardness	Gelcast (H_V, GPa)	Pellet (H_V, GPa)	Literature (values[19,20])
GOS	0.279	2.87	~8.8
Gd_2O_3	0.284	0.569	n.a.
Al_2O_3	14.84	12.97	18.63

Table 4
Density and porosity of sintered samples

	Gelcast (ρ, g/cm^3)	Gelcast (porosity, %)	Pellet (ρ, g/cm^3)	Pellet (porosity, %)
GOS	4.4	30.8	6.5	8.8
Gd_2O_3	4.9	39.2	5.9	37.2
Al_2O_3	3.9	1.4	3.7	9.1

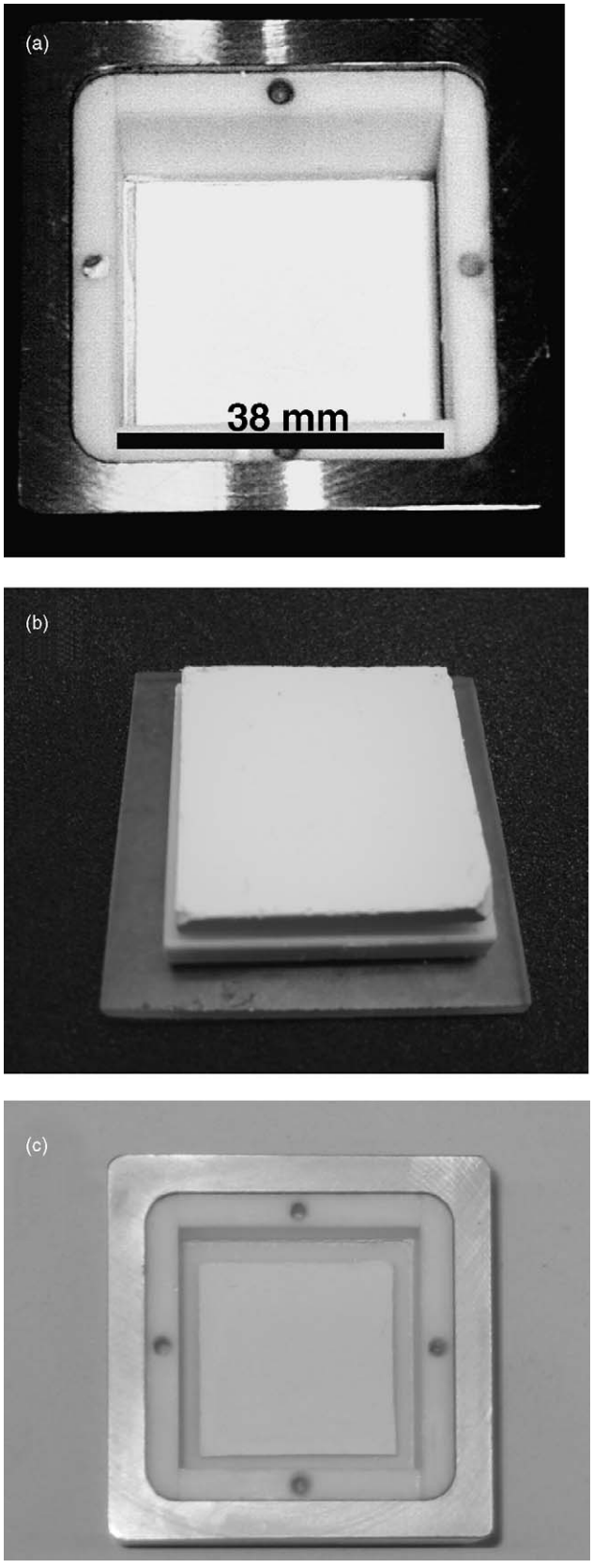

Fig. 9. Photograph of gelcast Gd_2O_2S, 25 vol.% (a) in a PTFE-mould, Gd_2O_3, 15 vol.% (b) removed from the PTFE-mould and Al_2O_3, 20 vol.% (c).

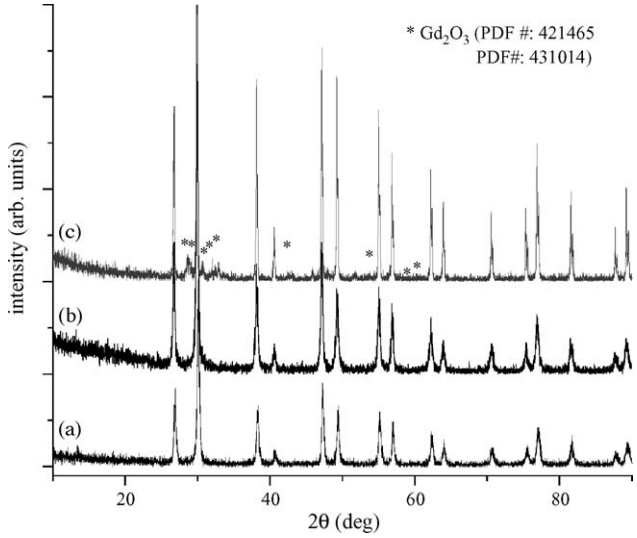

Fig. 10. XRD pattern of an as prepared (a), debindered (b) and sintered (c) Gd_2O_2S plate. The unlabeled peaks belong to Gd_2O_2S (PDF #: 261422).

Fig. 9a–c show photographs of gelcast, already polymerised Gd_2O_2S, Gd_2O_3 and Al_2O_3 parts, respectively, in a PTFE mould. The photographs of Gd_2O_3 and Al_2O_3 show gelcast plates removed from the PTFE mould.

The samples are dried in the mould at room temperature in a dynamic argon atmosphere to prevent surface cracking. Cracks appear usually because of the evaporation of EDA, which decomposes to different products. After ca. 60 h of steady argon flow rate the plates can be easily removed from the mould.

The XRD pattern in Fig. 10 of as prepared, debindered and sintered Gd_2O_2S plates shows no formation of a sulphate phase. The smaller signals belong predominately to Gd_2O_3, which might be formed due to the added $Gd(O_2CCH_3)_3$ compound. This leads to an excess of Gd^{3+} and will be transformed to the oxide during the debindering process.

In Fig. 11a and b, the SEM micrographs of gelcasted sintered Gd_2O_2S and Al_2O_3 samples, respectively, are shown. Fig. 12a shows a microscopic picture of a sintered Gd_2O_3 fibre and Fig. 12b and c show SEM pictures of a Gd_2O_3 fibre, which were made using a syringe with a 0.8 mm pin. The displayed samples were sintered at 1700 °C in air. However, the length of the fibres using a syringe is still limited to about 1–7 cm. The diameter of a fibre varies within 500–750 μm. Further test experiments with smaller syringe pins will be done, before investigations in a continuous laboratory apparatus will be started.

4. Discussion

Various parameters influence the polymerisation behaviour, including the time dependence of the gelcasting process. First of all the concentration of the CA monomer in the EDA solution is important. If it is too high, the complete dissolution of CA in EDA cannot take place. The whole mechanism can be understood by interpreting the ^{13}C NMR data. Cellulose acetate is formed by direct esterification of hydroxyl groups or by transesterification. By adding the compound to a strong base, such as EDA, the acetate group will be cleaved (deacetylation) and the gel will be formed (reaction A). The acetate group with the C(4) atom is transferred into the liquid. Therefore, the liquid contains $H_2NCH_2CH_3NH$ $OCCH_3$. Reactions B′ and B″ describe the mechanism, which occurs in the polymerisation step, initiated by adding metal ions, such as Gd^{3+} or Al^{3+}.

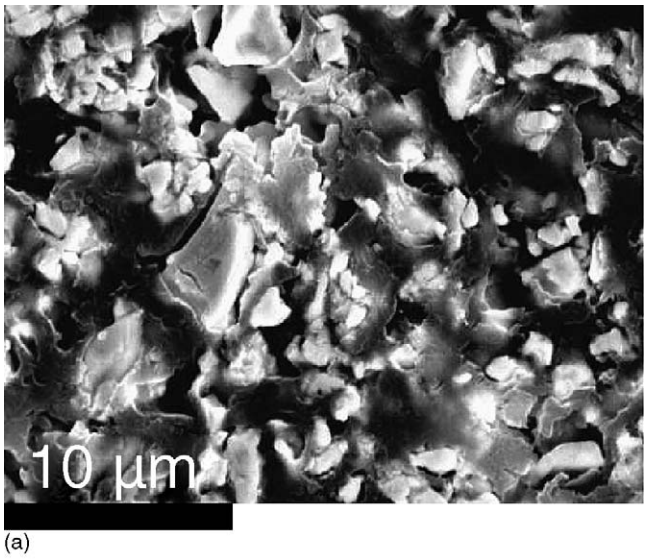

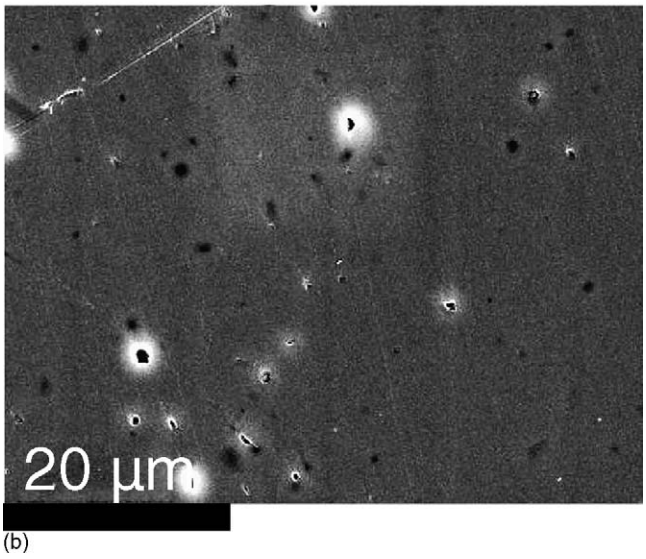

Fig. 11. (a) SEM micrograph of Gd_2O_2S gelcasted sample, powder concentration 25 vol.%. (b) SEM micrograph of Al_2O_3 gelcasted sample, powder concentration 25 vol.%.

$$\text{Cell-O}_2\text{CCH}_3 + \text{H}_2\text{NCH}_2\text{CH}_3\text{NH}_2 \rightarrow \text{cell-OH} + \text{H}_2\text{NCH}_2\text{CH}_2\text{NHOCCH}_3 \quad \text{(A)}$$

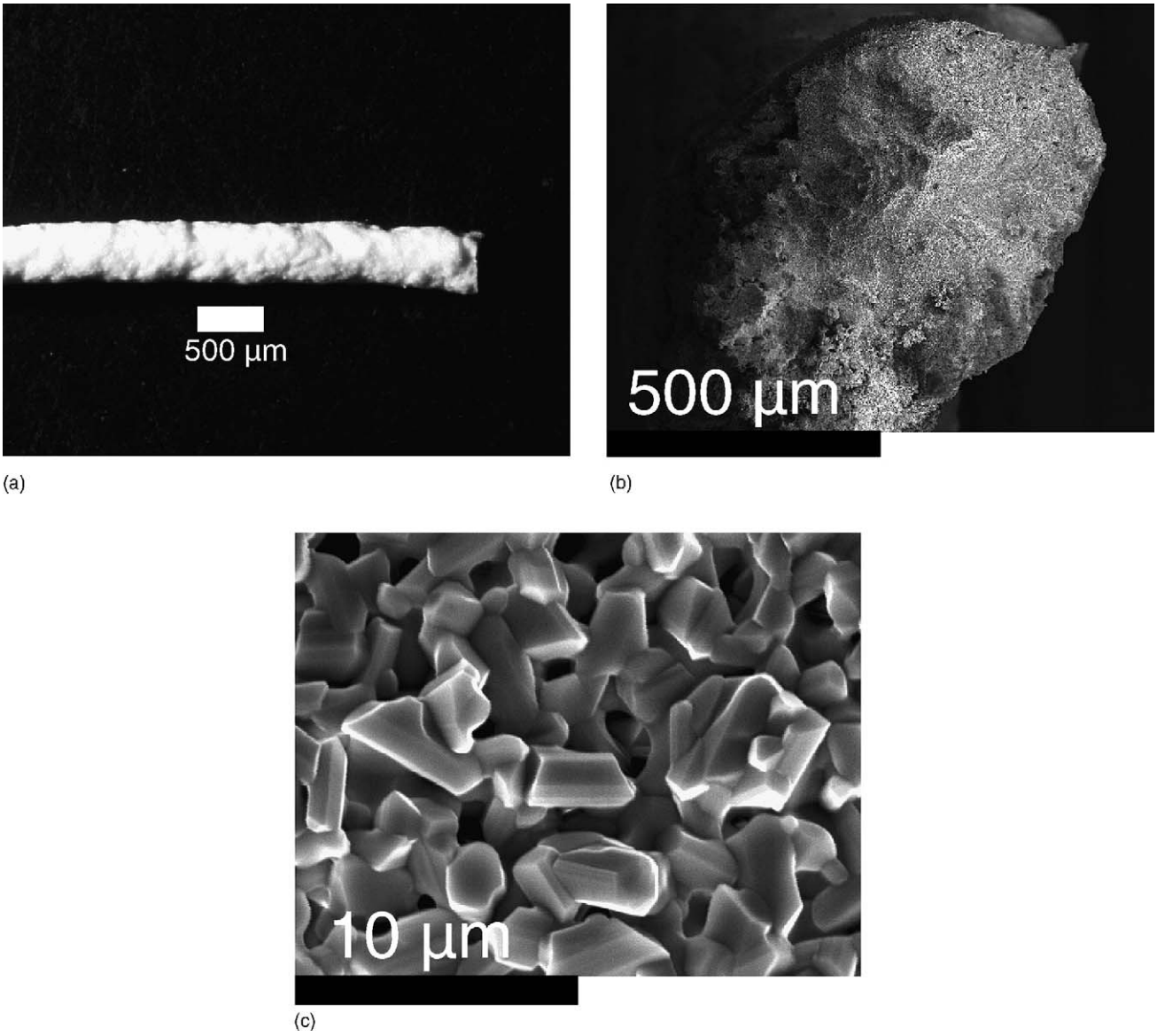

Fig. 12. (a) Optical stereomicroscope image of a Gd_2O_3 fibre sintered at 1700 °C in air, powder concentration 25 vol.%. (b) Fracture of a Gd_2O_3 fibre sintered at 1700 °C in air. (c) Detailed view of the same sample, where clearly the sinter necks are visible.

$$\text{Cell-OH} + \text{H}_2\text{NCH}_2\text{CH}_2\text{NH}_2 \rightarrow \text{cell-O}^- + \text{H}_2\text{NCH}_2\text{CH}_2\text{NH}_3^+ \quad (\text{B}')$$

$$\text{cell}\text{—}\text{O}^- + \text{M}^{3+} \longrightarrow \begin{matrix} \text{cell-O} & & \text{O-cell} \\ & \text{M} & \\ & \text{O-cell} & \end{matrix} \quad (\text{B}'')$$

The second parameter is the concentration of metal ions as initiator. Above a certain concentration level (0.5–1.0 wt.%) the amount of free metal ions is too high and will not contribute anymore to an accelerated polymerisation. The slurry is basically "supersaturated" by the initiator cations. Furthermore, acetone causes a slower network formation of the free metal cations, which are responsible for the gelation behaviour, that is free "cellulose anions" in an acetone solution cannot build up the stable network with the free metal cations. The higher the added volume of acetone is, the slower the polymerisation starts, therefore, more free cellulose anions in the slurry are present. The third point is the powder weight fraction in the slurry. Besides the influence on the viscosity of the slurry, which increases with higher powder loads, there is a dependence of the powder load on the gelation time. The dispersibility is decreased, and therefore, an increase of gelation time occurs because of interaction of different ζ-potentials of the powder both with cellulose acetate and free cations as well as different grain sizes and their distribution. Since the ζ-potential of Al_2O_3 is very different from the Gd_2O_3 and Gd_2O_2S powders, there are also different maximum powder loads for the gelcasting slur-

ries. Much more powder of Al_2O_3, namely 40 vol.%, can be dispersed in the CA/EDA solution, but only approximately 30 vol.% of Gd_2O_3 or Gd_2O_2S can be dispersed into the solution without reducing the flowability by a viscosity too high to cast the slurry into the mould.

Besides the optimum slurry parameters the drying process of the casted slurry is very important. The effect of atmosphere type on the gelcasting behaviour is also reported in literature (e.g.[17,18]). If the plate will be stored in air, always cracks on the surface appear after a few hours. They result from the EDA decomposition products,[11] mainly degassing ammonia (NH_3), which causes surface stresses. In argon or dried nitrogen atmosphere this process is delayed, NH_3 forms very slowly and can completely leave the plate without causing surface cracks. When the EDA content in the plate has reached a low level after 60 h, the degassing of the residual solvent does not cause cracks any more. The whole drying process has to be applied for the extruded fibres as well.

Although the green density of gelcast plates is lower than for uniaxially pressed pellets, it can be seen that simple casting in a mould without applying pressures results in quite dense and stable green bodies. The same can be concluded from the pore size data obtained from BET measurements. The values are almost consistent with the values for the pellets. The reason for the differences in the pore diameter measured by mercury intrusion is the higher compaction of uniaxially pressed pellets. Applying pressure can reduce larger pores. This has an effect on debindered pellet samples as well and can almost be balanced in the sintering step where open pores in the gelcast pellets can drastically be reduced as the values for Al_2O_3 demonstrate.

5. Conclusions

This work shows results for a gelcasting method, which uses cellulose acetate as monomer and a non-aqueous solvent, ethylenediamine, and gives, therefore, the possibility to process moisture-sensitive ceramic powders. Here, we investigated a Gd_2O_2S ceramic powder as an example for such sensitive ceramics. Essential and basic experiments have been done in terms how to influence the polymerisation time and the viscosity of different ceramic slurries. The results show the possibility to make ceramic plates and fibres using this gelcasting method, without applying pressure to form different body shapes, including fibres.

Acknowledgements

We gratefully acknowledge the help of Dr. L. Heymann and G. Jena, Department of Applied Mechanics and Fluid Dynamics, University of Bayreuth, for the rheological measurements. Further, we thank Dipl.-Chem. Xavier André, Department of Molecular Chemistry II, University of Bayreuth, for the ^{13}C NMR measurements.

References

1. Omatete, O. O., Janney, M. A. and Strehlow, R. A., Gelcasting – a new ceramic forming process. *Bull. Am. Ceram. Soc.*, 1991, **70**(10), 1641–1649.
2. Baskin, D. M., Zimmerman, M. H., Faber, K. T. and Fuller Jr., E. R., Forming single-phase laminates via the gelcasting technique. *J. Am. Ceram. Soc.*, 1997, **80**(11), 2929–2932.
3. Omatete, O. O., Janney, M. A. and Nunn, S. D., Gelcasting: from laboratory development toward industrial production. *J. Eur. Ceram. Soc.*, 1997, **17**, 407–413.
4. Zimmerman, M. H., Faber, K. T. and Fuller Jr., E. R., Forming textured microstructures via the gelcasting technique. *J. Am. Ceram. Soc.*, 1997, **80**(10), 2725–2729.
5. Janney, M. A., Omatete, O. O., Walls, C. A., Nunn, S. D., Ogle, R. J. and Westmoreland, G., Development of low-toxicity gelcasting systems. *J. Am. Ceram. Soc.*, 1998, **81**(3), 581–591.
6. Janney, M. A., Nunn, S. D., Walls, C. A., Omatete, O. O., Ogle, R. B., Kirby, G. H. *et al.*, Gelcasting. In *The handbook of ceramic engineering*, ed. M. N. Rahaman. Marcel Dekker, Oak Ridge, TN, 1998.
7. Tarì, G., Gelcasting ceramics: a review. *Bull. Am. Ceram. Soc.*, 2003, **82**(4), 43–46.
8. Cai, K., Huang, Y. and Yang, J., Alumina gelcasting by using HEMA. *J. Eur. Ceram. Soc.*, 2005, **25**(7), 1089–1093.
9. http://www.ikts.fraunhofer.de/, 2005.
10. http://www.ornl.gov/info/ornlreview/rev28-4/text/gelcast.htm, 2005.
11. Vollhardt, K. P. C. and Schore, N. E., *Organische Chemie*, *vol. 3*. Wiley-VCH, 2000, p. 1477.
12. Yamada, H. H., Tsukuda, Y. O., Suzuki, A. H., Yamamoto, H., Yoshida, M., Maio, K. *et al.*, *Szintillatorkörper für einen Strahlungsdetektor*, 1987, DE 3629180 C2, p. 7.
13. Leppert, J. and Rossner, W., *Ger. Offen. Verfahren zur Herstellung einer Szintillationskeramik*, 1994, DE 4224931 A1, p. 7.
14. Leppert, J., *Ger. Offen. Verfahren zur Herstellung von Szintillationskeramik*, 2000, DE 19913545 C1, p. 4.
15. Suponitskii, Y., Laptev, V. I. and Vorob'ev, A. F., Thermal oxidation of lanthanide oxysulfides. *Zhurnal Neorganicheskoi Khimii*, 1989, **34**(10), 2690–2693.
16. Fayou, Yu, *Development of a gelcasting process for thin scintillator ceramic plates*. Diplomarbeit, Fakultät für Angewandte Naturwissenschaften, Lehrstuhl für Werkstoffverarbeitung, Universität Bayreuth, 2001, p. 84.
17. Ha, J.-S., Effect of atmosphere type on gelcasting behavior of Al_2O_3 and evaluation of green strength. *Ceram. Int.*, 2000, **26**, 251–254.
18. Barati, A., Kokabi, M. and Navid Famili, M. H., Drying of gelcast ceramic parts via the liquid desiccant method. *J. Eur. Ceram. Soc.*, 2003, **23**, 2265–2272.
19. Numazawa, T., Yanagitani, T., Nozawa, H., Ikeya, Y., Li, R. and Satoh, T., In *A new ceramic magnetic regenerator material for 4 K cryocoolers*. Kluwer Academic/Plenum Publishers, Cambridge, MA, 2002.
20. http://www.quick-ohm.de/keramik/ceramic_kugel.html, 2005.